Role of Osteoblast–Fibroblast Interactions in the Formation of the Ligament-to-Bone Interface

I-Ning E. Wang,[1] Jing Shan,[1] Rene Choi,[1] Seongcheol Oh,[1] Christopher K. Kepler,[1] Faye H. Chen,[2] Helen H. Lu[1,3]

[1]Biomaterials and Interface Tissue Engineering Laboratory, Department of Biomedical Engineering, Columbia University, 1210 Amsterdam Avenue, 351 Engineering Terrace Building, MC 8904, New York, New York 10027

[2]Cartilage Biology and Orthopaedics Branch, National Institute of Arthritis and Musculoskeletal and Skin Diseases, National Institutes of Health, Department of Health and Human Services, Bethesda, Maryland 20892

[3]College of Dental Medicine, Columbia University, New York, New York 10032

Received 9 March 2007; accepted 18 May 2007

Published online 3 August 2007 in Wiley InterScience (www.interscience.wiley.com). DOI 10.1002/jor.20475

ABSTRACT: The anterior cruciate ligament (ACL) inserts into bone through a characteristic fibrocartilagenous interface, which is essential for load transfer between soft and hard tissues. This multi-tissue interface is lost post ACL reconstruction, and the lack of an anatomic fibrocartilage interface between graft and bone remains the leading cause of graft failure. Currently, the mechanism of interface formation is not known. As a fibrocartilage-like tissue is found within the bone tunnel post ACL reconstruction, we hypothesize that fibroblast–osteoblast interactions at the graft-to-bone junction play a role in fibrocartilage formation. To test this hypothesis, a co-culture model permitting osteoblast–fibroblast communications was used to determine the effects of heterotypic interactions on cell phenotype and the development of fibrocartilage-relevant markers in vitro. It was found that co-culture decreased cell proliferation and osteoblast-mediated mineralization, while inducing fibroblast-mediated mineralization. Moreover, the expression of interface-relevant markers such as collagen type II and aggrecan were detected. Our findings suggest that osteoblast–fibroblast interactions may lead to cell trans-differentiation and eventual fibrocartilage formation. These results provide new insight into the mechanism of fibrocartilage formation, which are critical for interface tissue engineering and achieving biological fixation of soft tissue grafts to bone. © 2007 Orthopaedic Research Society. Published by Wiley Periodicals, Inc. J Orthop Res 25:1609–1620, 2007

Keywords: fibrocartilage; interface; enthesis; co-culture; fibroblasts

INTRODUCTION

The anterior cruciate ligament (ACL) is a dense connective tissue that joins the femur to the tibia, and serves as the primary knee joint stabilizer. It inserts into subchondral bone through a characteristic fibrocartilage interface, with controlled spatial variation in cell type and matrix composition.[1–8] Due to mechanical graft fixation, the anatomic insertion site is not regenerated post ACL reconstruction.[9,10] Without this interface, mechanical stability is limited at graft-bone junction[9,11] and the lack of biological fixation remains the primary cause of graft failure.[9,12–14]

The ACL-to-bone interface consists of three distinct tissue regions: ligament, fibrocartilage, and bone. The fibrocartilage region is further divided into the non-mineralized and mineralized fibrocartilage zones. The ligament proper comprises of fibroblasts embedded in a matrix rich in collagen types I and III. The non-mineralized fibrocartilage zone consists of ovoid chondrocytes, and collagen types I and II are detectable within the proteoglycan-rich matrix. The next region is the mineralized fibrocartilage zone, with hypertrophic chondrocytes surrounded by a mineralized matrix containing collagen type X.[6,15] The last region is the subchondral bone, within which osteoblasts, osteocytes, and osteoclasts are embedded in a mineralized collage type I matrix. This multi-tissue, controlled matrix heterogeneity is important for minimizing stress concentrations and facilitating the transfer of complex loads between soft and hard tissues.[2,16,17]

Currently, the mechanism governing interface formation is not known. There is, however, evidence that this interface may be regenerated.

Correspondence to: Helen H. Lu (Telephone: 212-854-4071; Fax: 212-854-8725; E-mail: hl2052@columbia.edu)

When the Achilles tendon is sutured to its original attachment site, cellular organization resembling that of the native insertion and type X collagen deposition were observed.[18] In addition, even though tendon-to-bone healing following ACL reconstruction does not lead to the re-establishment of the anatomic insertion, a fibrovascular tissue is formed within the bone tunnel.[10,19–21] While both the location and orientation of this neo-fibrocartilage are non-anatomical, these observations suggest that a fibrocartilage-like tissue can be regenerated between soft tissue and bone in vivo. Moreover, this tissue is formed in regions at which the graft is in direct contact with bone, suggesting that interactions between cells derived from tendon (e.g., fibroblasts) and bone tissue (e.g., osteoblasts) play a role in fibrocartilage formation by initiating phenotypic changes or trans-differentiation of osteoblasts and/or fibroblasts.

To test this hypothesis, the first objective of this study is to design a biomimetic osteoblast–fibroblast co-culture model which will facilitate physical contact and paracrine interactions, as well as mimicking the multi-cellular organization at the native graft-to-bone interface. As this is, to our knowledge, the first reported study to examine the interaction of osteoblasts and ACL fibroblasts, the second study objective is to identify the optimal media conditions for co-culturing. Specifically, ascorbic acid (AA) and β-glycerophosphate (βGP) concentrations are optimized to encourage cell growth, and minimize fibroblast calcification without compromising osteoblast-mediated mineralization. The next study objective is to evaluate the effects of co-culture on the growth and phenotype maintenance of osteoblasts and fibroblasts. The development of insertion-relevant markers[8] such as glycosaminoglycans, cartilage oligomeric matrix protein (COMP), collagen types I, II, and X in co-culture will be determined. Finally, our model is further optimized in order to discern the response of cell subpopulations (e.g., osteoblasts or fibroblasts) in co-culture. It is anticipated that findings of this study will provide new insight into the mechanism for fibrocartilage formation.

MATERIALS AND METHODS

All chemicals were purchased from Sigma Chemical (St. Louis, MO) unless otherwise noted.

Cells and Cell Culture

Primary fibroblasts and osteoblasts were obtained from explant cultures of anterior cruciate ligament[22] and trabecular bone fragments[23] harvested from neonatal calves (Fresh Farm, Rutland, VT). The ligament was excised from the joint after removing the synovial sheath, while trabecular bone fragments were cored from subchondral bone. For explant cultures, the tissue was minced and incubated in Dulbecco's Modified Essential Medium (DMEM) with 10% fetal bovine serum, 1% non-essential amino acids, and 1% antibiotics (Mediatech, Herdon, VA). Cell outgrowth was observed after 1 week, and cells derived from the second/third migration were used based on published protocols.[22,24,25] The cultures were grown to confluence at 37°C and 5% CO_2.

Osteoblast–Fibroblast Co-Culture Model

The osteoblast and fibroblast co-culture model (Fig. 1) was established by first forming a permeable hydrogel divider (~5 mm in width, 4% agarose) within a tissue culture well (surface area ~400 mm^2). As shown in Figure 1, osteoblasts were seeded on the right and fibroblasts on the left of the divider, each at 5×10^4 cells/section. Media was added after allowing the cells to attach for 30 min, with the culture well including the divider covered with media. The cells were co-cultured in this configuration for 1 week, after which the divider was removed, and both cell types migrated into and interacted directly within the interface zone. Cell distribution, in particular the relative positions and subsequent interaction between these cells in co-culture were monitored by pre-labeling fibroblasts with the CellTracker CM-DiI (Molecular Probes, Eugene, OR) and osteoblasts with Vybrant CFDA SE Cell Tracer (Molecular Probes) following the manufacturer's protocols. Cell distribution was imaged by fluorescence microscopy (Carl Zeiss, Jena, Germany).

Effects of Medium Additives on Osteoblast and Fibroblast Response

The second objective of this study was to formulate an optimal co-culture medium by determining the effects of ascorbic acid (AA) and β-glycerophosphate (βGP) on osteoblast and fibroblast responses. Specifically, individual cultures of each cell type (1.5×10^4 cells/cm^2) were established in fully supplemented DMEM. The effects of media AA concentration ([AA], 0, 10, 50, 100 μg/ml) and βGP concentration ([βGP], 0, 1.0, 3.0, 5.0 mM) on cell growth ($n = 5$) and mineralization ($n = 5$) were determined as a function of time for both osteoblasts (1, 3, 7, 14 days) and fibroblasts (1, 3, 7 days). The AA solution was freshly prepared during each media exchanges.

Effects of Co-Culture on Overall Cell Growth and Differentiation

The third objective of this study focuses on the effects of osteoblast and fibroblast co-culture on cell growth, alkaline phosphatase (ALP) activity, mineralization, glycosaminoglycan (GAG) production, and gene expression. Fibroblast-only and osteoblast-only groups served

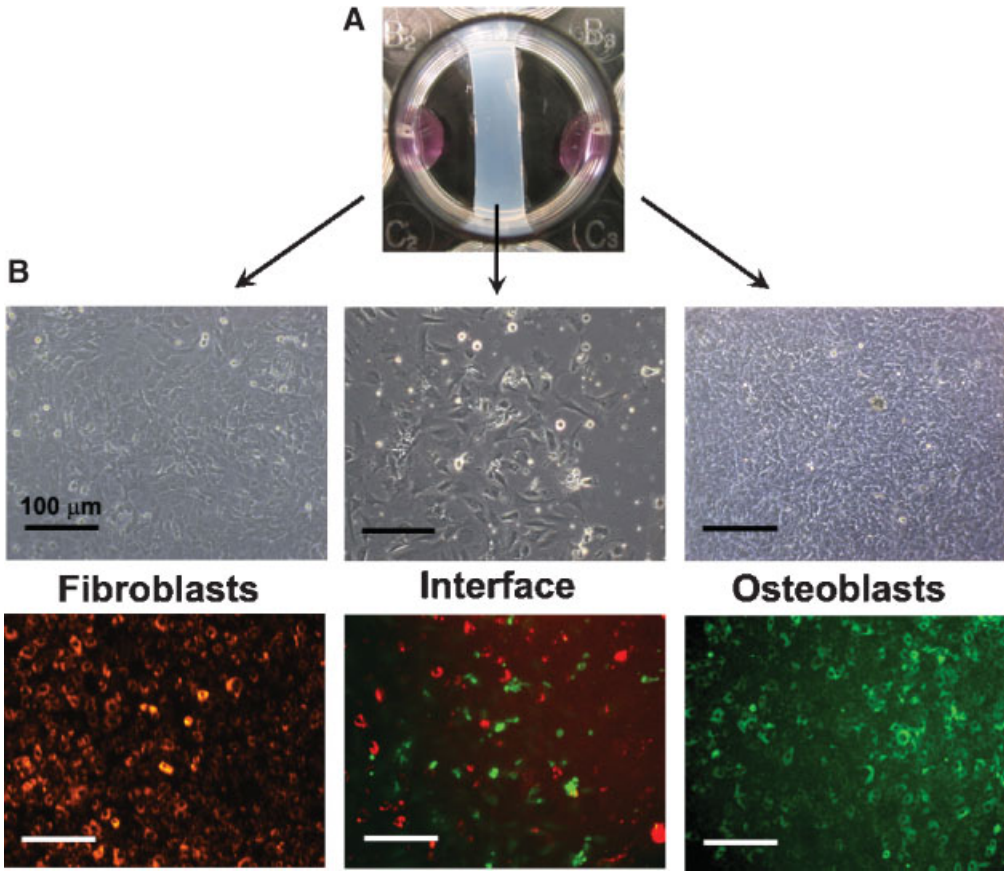

Figure 1. Co-culture model of fibroblasts and osteoblasts. The co-culture model is formed by first dividing the well into three regions, with fibroblast on the left, osteoblasts on the right, and an interface region defined initially with a hydrogel divider. The hydrogel insert separates the two cell types and permits paracrine interaction during the first week of co-culture. The divider was removed at day 7 and physical interaction was permitted between osteoblast and fibroblasts. (A) An image of the co-cultured well after initial cell seeding. (B) Light micrographs and corresponding fluorescence images of the fibroblast, osteoblast, and interface regions at day 14. Three distinct regions are established: fibroblasts (red, CM-DiI), osteoblasts (green, CFDA-SE), as well as fibroblasts + osteoblasts at the interface region.

as controls. The co-culture medium was supplemented with optimized [AA] and [βGP]. In addition, the effect of co-culture ratio on overall cell proliferation was examined. Specifically, three fibroblast:ostoblast ratios were tested: 1:1 which has 5×10^4 fibroblasts and 5×10^4 osteoblasts; 1:2 which has 5×10^4 fibroblasts and 10×10^4 osteoblasts; and 2:2 which has 10×10^4 fibroblasts and 10×10^4 osteoblasts.

Optimization of the Co-Culture Model: Response of Cell Subpopulations in Co-Culture

In order to determine the effects of co-culture on the response of cell subpopulations (osteoblasts, fibroblasts, osteoblasts + fibroblasts at the interface), we further optimized the co-culture model shown in Figure 1. Briefly, instead of directly seeding each cell type on their respective side of the well, osteoblasts (5×10^4 cells) or fibroblasts (5×10^4 cells) were pre-seeded for 30 min on Thermanox coverslips (Fisher Scientific, Fair Lawns, NJ). The fibroblast- or osteoblast-seeded coverslips were subsequently fixed on their respective side of the hydrogel divider, and the two cells types were grown in the optimized co-culture media over time. Similar to the previous model, the divider was removed at day 7 to permit direct osteoblast–fibroblast interactions. At each time point (1, 4, 7, and 14 days), the coverslips from the fibroblast or osteoblast regions of the co-cultured well, as well as the cells in the interface region were removed and analyzed separately. The proliferation, ALP activity, and gene expression of each cell subpopulation in co-culture (Ob in co-culture, Fb in co-culture, Co-culture interface) were assessed.

Cell Proliferation

Total DNA per sample ($n = 6$) was measured using the PicoGreen® dsDNA assay (Molecular Probes) following the manufacturer's suggested protocol. Briefly, at each time point, cells were lysed with 0.1%

Triton-X100 and collected using a cell scraper. The amount of DNA/sample was correlated to fluorescence intensity measured with a microplate reader (Tecan, Maennedorf, Switzerland), at the excitation and emission wavelengths of 485 nm and 535 nm, respectively.

Alkaline Phosphatase (ALP) Activity and Mineralization

Sample alkaline phosphatase (ALP) activity was assessed using both quantitative[26] and qualitative methods.[26] Quantitative ALP activity ($n = 6$) was measured using an enzymatic assay based on the hydrolysis of p-Nitrophenyl phosphate (pNP-PO_4) to p-nitrophenol (pNP). Briefly, the cells were lysed with 0.1% Triton-X100 solution and collected using a cell scraper. The samples were incubated at 37°C for 30 min in 0.1 M Na_2CO_3 buffer containing 2 mM $MgCl_2$, with pNP-PO_4 as the substrate. Standards were based on 0.5 mM p-nitrophenol (pNP). Absorbance was measured at 405 nm, and enzymatic activity was expressed in total μM of pNP/min. The distribution of ALP activity ($n = 3$) was ascertained by Fast-Blue staining after fixing the samples with neutral buffered formalin. The samples were incubated in ALP staining solution for 30 min and washed with deionized water before imaging. Alizarin Red S (ALZ) staining[26] was used to visualize mineral deposition ($n = 3$). Briefly, after fixation in 95% ethanol, the samples were incubated in 2% ALZ for 10 min, washed with deionized water, and imaged by light microscopy.

Sulfated Glycosaminoglycan (GAG) Deposition and Gene Expression

Glycosaminoglycan (GAG) deposition was visualized by Alcian Blue staining.[8] Briefly, the samples ($n = 3$) were fixed with acid-formalin for 10 min at each time point. After rinsing with phosphate buffered saline, the samples were incubated overnight with 1.0% of Alcian Blue dye. Dark blue stain is indicative of positive GAG staining.

Gene expression was measured by reverse transcription followed by polymerase chain reaction (RT-PCR). Primers were designed for collagen type I (TGCTGGCCAACCATGCCTCT, TTGCACAATGCTCTGATC); type II (ATGACAACCTGGCTCCCAAC, GCCCTATGTCCACACCGA); aggrecan (CACTGTTACCGCCACTTCCC,GACATCGTTCCACTCGCCCT); and GAPDH (GGTGATGCTGGTGCTGAGTA, ATCCACAGTCTTCTGGGTGG).[25,27,28] Total RNA was isolated ($n = 2$) using the Trizol® extraction method (Invitrogen, Carlsbad, CA). The isolated RNA was reverse transcribed into cDNA using the SuperScript™ First-Strand Synthesis System, and amplified using recombinant Taq DNA polymerase. All genes were amplified for 40 cycles in a thermal cycler (Brinkmann, Westbury, NY), and analyzed by gel electrophoresis. Semi-quantitative result was obtained using ImageJ software. Gene expression was normalized by GAPDH. In addition, gene expression of interface-relevant markers at the interface region in the optimized model was quantified by real-time PCR ($n = 3$) using iQ SYBR Green Supermix (BioRad, Hercules, CA) and iCycler iQ Real-Time PCR Detection System (BioRad).[28] Specific gene expression was first normalized to GAPDH and then compared to the control groups.

Statistical Analysis

Data are presented as the mean ± standard deviation. A two-way analysis of variance (ANOVA) was performed to determine the effects of co-culture and time on cell number and ALP activity. The Tukey-Kramer post hoc test was used for all pair-wise comparisons and statistical significance was set at $p < 0.05$. All statistical analyses were performed using the JMP statistical software package (SAS Institute, Cary, NC).

RESULTS

Osteoblast–Fibroblast Co-Culture Model

The co-culture model (Fig. 1) was designed to emulate the in vivo condition when the soft tissue graft is placed directly adjacent to bone tissue within the bone tunnel. This biomimetic model permits both physical contact and paracrine interaction between both cell types. Osteoblasts and fibroblasts were separated by a hydrogel divider during the first week of co-culture, allowing the cultures to equilibrate and grow to confluence prior to direct physical contact. When the divider was removed at day 7, the cellular regions adjacent to either side of the divider have become confluent. Cell tracking results demonstrate that both fibroblasts and osteoblasts rapidly migrated into the interface region after day 7 (Fig. 1B). Moreover, fibroblasts (in red) and osteoblasts (in green) were localized in their respective regions before and after divider removal. At the end of the experiment, three regions were thus established: fibroblast-only, fibroblast plus osteoblast, and osteoblast-only (Fig. 1B), with each consisting of the dominant cell type found at the graft-bone interface.

Optimization of Medium Additive Concentration for Co-culture

To maximize cell growth and osteoblast calcification, while minimizing ectopic fibroblast mineralization, optimal [AA] and [βGP] were determined. For osteoblasts, the highest cell number was measured at 10 μg/ml [AA] (Fig. 2A). Similarly, this [AA] was also optimal for fibroblast proliferation (Fig. 2B, $p < 0.05$). Staining with ALZ revealed that osteoblast and fibroblast mineralization increased with [AA], with the lowest fibroblast mineralization seen at 0 and 10 μg/ml [AA] (data not shown). Consequently, the optimal [AA] for co-culture was chosen at 10 μg/ml.

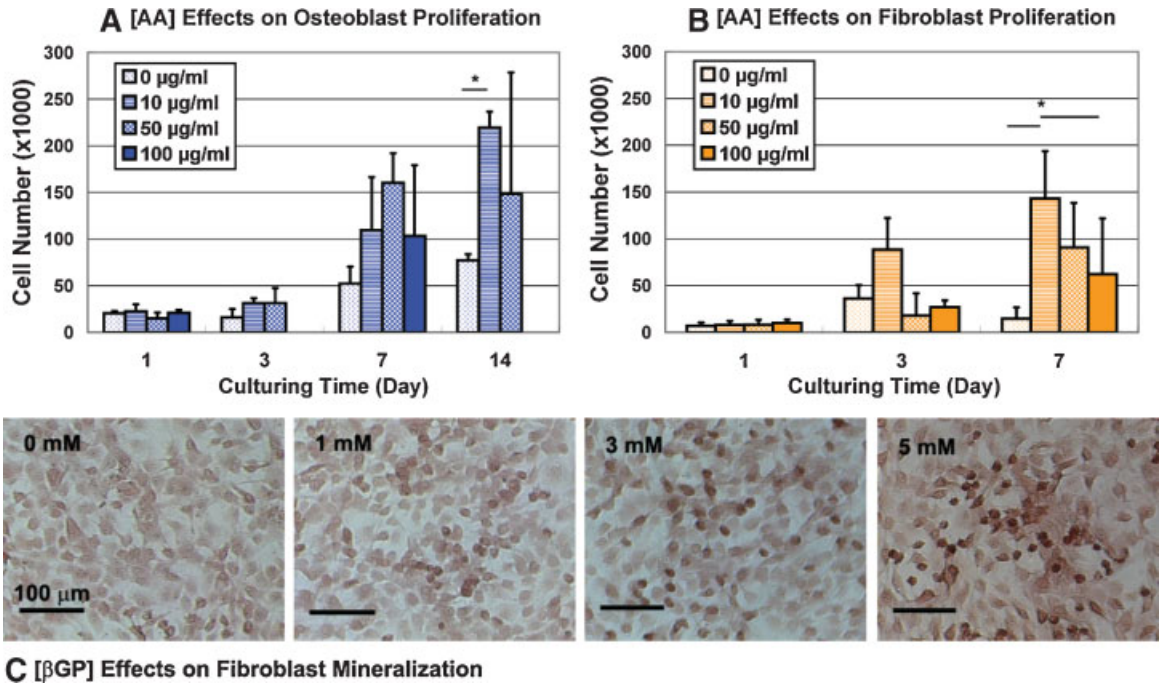

Figure 2. Effects of L-ascorbic Acid ([AA]) and β-glycerolphosphate concentrations ([βGP]) on osteoblast and fibroblast proliferation and mineralization. Highest cell number was found at [AA] of 10 µg/ml, and [βGP] of 1 mM resulted in the lowest fibroblasts-mediated mineralization. (A) Osteoblast proliferation with increasing [AA]. (B) Fibroblast proliferation with increasing [AA]. (C) Alizarin S (ALZ) staining for fibroblast mineralization with increasing [βGP], day 14. (* denotes significance at $p < 0.05$).

Increased cell mineralization was observed with increasing [βGP] in both osteoblast and fibroblast cultures. All concentrations (1, 3, 5 mM) were found to support osteoblast mineralization (data not shown), while stronger ALZ stain intensity was observed for fibroblast cultures of 3.0 mM or higher (Fig. 2C). At day 14, a significant higher number of cells was found at 1.0 mM when compared to 3.0 mM of [βGP] (data not shown). Balancing the need for osteoblast mineralization without increasing fibroblast calcification, 1.0 mM was selected as the optimal [βGP] for co-culture.

Effects of Co-Culture on Cell Growth

The cells in co-culture entered the exponential phase after 3 days, and cell growth plateaued after 14 days (Fig. 3A). Fibroblast- and osteoblast-only cultures exhibited similar growth profiles, with a 24% lower doubling time for fibroblasts than osteoblasts (fibroblasts = 1.45 days, osteoblasts = 1.91 days). The doubling time for co-culture was 1.96 days, reflecting an over 35% decrease in growth rate when compared to the fibroblast control group. When the fibroblast:osteoblast ratio is changed to 1:2, a decrease in total cell number in co-culture was observed, while a similar growth pattern was observed at the 1:1 and 2:2 co-culture ratios (Fig. 3B).

Effects of Co-Culture on Alkaline Phosphatase Activity and Mineralization

The ALP activity in the osteoblast-only control peaked at day 14 and decreased thereafter (Fig. 4A), while the fibroblast-only group exhibited a basal level of ALP activity over time. In co-culture, the ALP activity was significantly lower at day 14 and reached a maximum at day 28. Qualitative ALP staining results confirm these observations, with osteoblasts in co-culture stained less intensely for ALP activity than the osteoblast-only control (Fig. 4B). In contrast, fibroblasts in co-culture stained increasingly positive for ALP when compared to the fibroblast-only control (Fig. 4B, C). Cell tracking results (Fig. 4C) confirmed that in co-culture, the ALP-positive cells found at the fibroblast side did not originate from the osteoblast side of the co-cultured well.

For mineralization, positive staining for calcium was observed in the osteoblast control group

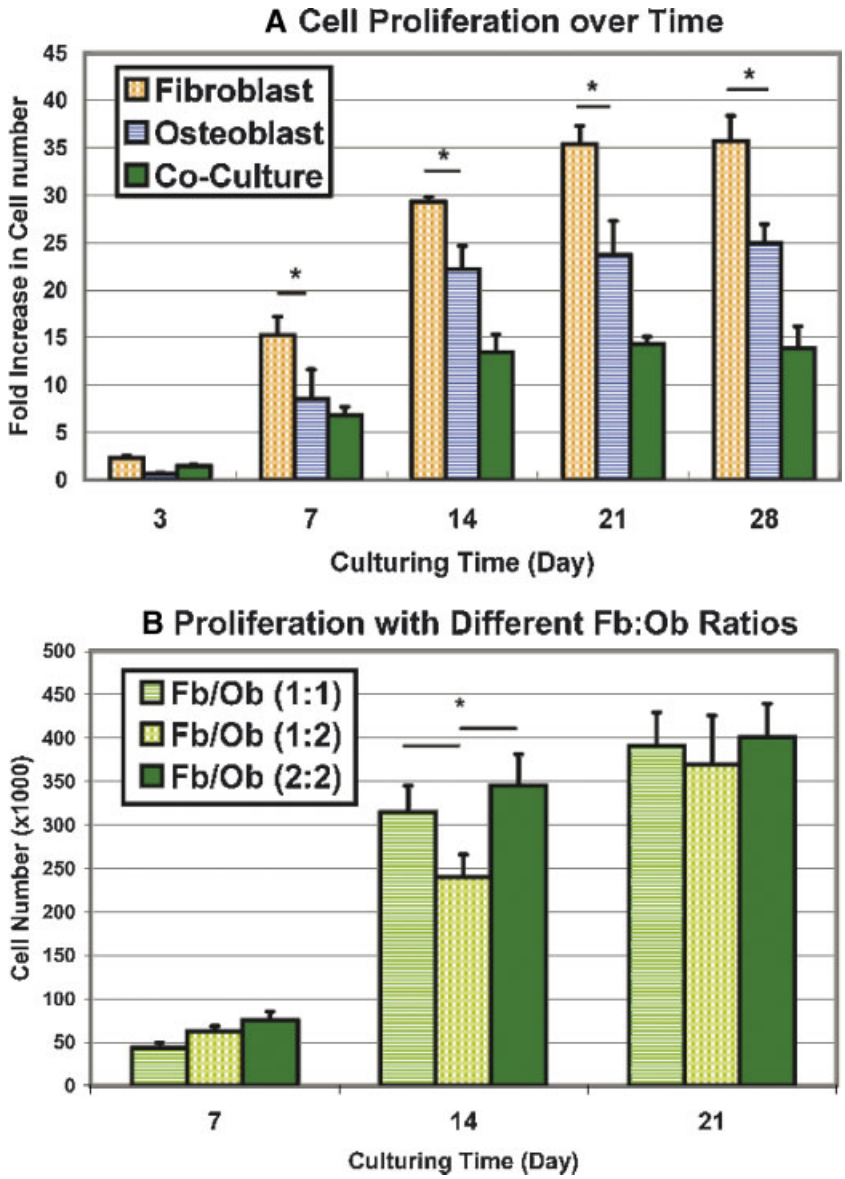

Figure 3. Effects of co-culture on cell proliferation. Co-culture suppressed overall cell proliferation when compared to individual cultures of osteoblasts or fibroblasts. Fibroblast growth was consistently higher than that of osteoblasts. (A) Fold increase in cell number compared to day 1. (B) Cell proliferation as a function of different co-culture ratios of fibroblasts (Fb) to osteoblasts (Ob). (* denotes significance at $p < 0.05$).

(Fig. 5A), while background staining was seen in the fibroblast control. In co-culture, ALZ staining intensity at the fibroblast side of the co-cultured well remained relatively low, while a decrease in stain intensity on the osteoblast side was observed over time.

Effects of Co-Culture on the Development of Interface-Specific Markers

The development of interface-relevant markers such as aggrecan and collagen type II was determined as a function of co-culture. Qualitative Alcian Blue staining revealed little change in GAG production due to co-culture, as only background staining was observed (data not shown). The co-cultured group as well as the osteoblast and fibroblast controls consistently expressed collagen type I and aggrecan (aggrecan data not shown). Interestingly, co-culture of osteoblasts and fibroblasts resulted in elevated expressions of collagen type II and COMP after 28 days (Fig. 5B). Expression of collagen type X was not detected in the co-cultured or control groups.

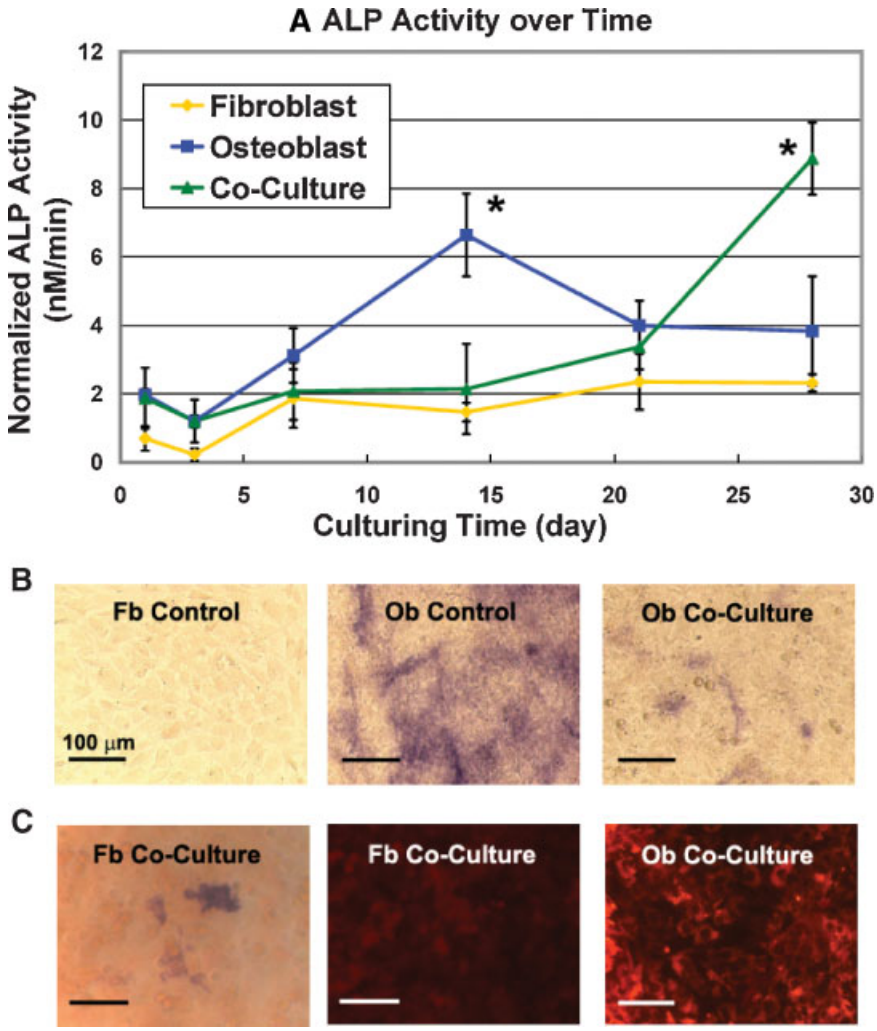

Figure 4. Effects of co-culture on alkaline phosphatase (ALP) activity. The ALP activity of osteoblasts (Ob) decreased in co-culture while those of fibroblasts (Fb) increased. (A) Normalized ALP activity over time. (B) ALP activity (Fast-Blue staining) of the co-cultured osteoblasts and control groups, day 14. (C) Fluorescence tracking of osteoblasts (red, CM-DiI) revealed that the positive ALP staining seen in the fibroblast region of the co-cultured well was not associated with osteoblasts. (* denotes significance at $p < 0.05$).

Optimization of the Co-Culture Model

As shown in Figure 6A, a similar suppression of osteoblast as well as fibroblast proliferation due to co-culture was observed at day 14 in the optimized model. Moreover, osteoblast ALP activity in co-culture was significantly lower than that of osteoblast control at day 7, while minimal fibroblast ALP activity due to co-culture was measured (Fig. 6B). While no significant changes were detected in osteoblast gene expression in co-culture, real-time PCR results (Fig. 6C) revealed that the fibroblast side of the well in co-culture down-regulated the expression for collagen type II and aggrecan. The interface region in co-culture showed up-regulation of both genes due to osteoblast–fibroblast interactions.

DISCUSSION

Our long term goal is to elucidate the mechanism for regenerating the ligament-to-bone interface, and this study focuses on the role of heterotypic cellular interactions in this process. A biomimetic co-culture model was designed and then optimized to evaluate osteoblast–fibroblast interactions and the relevance of these communications in interface formation. A hydrogel divider was first used to facilitate cell localization within the desired regions while allowing paracrine interactions via

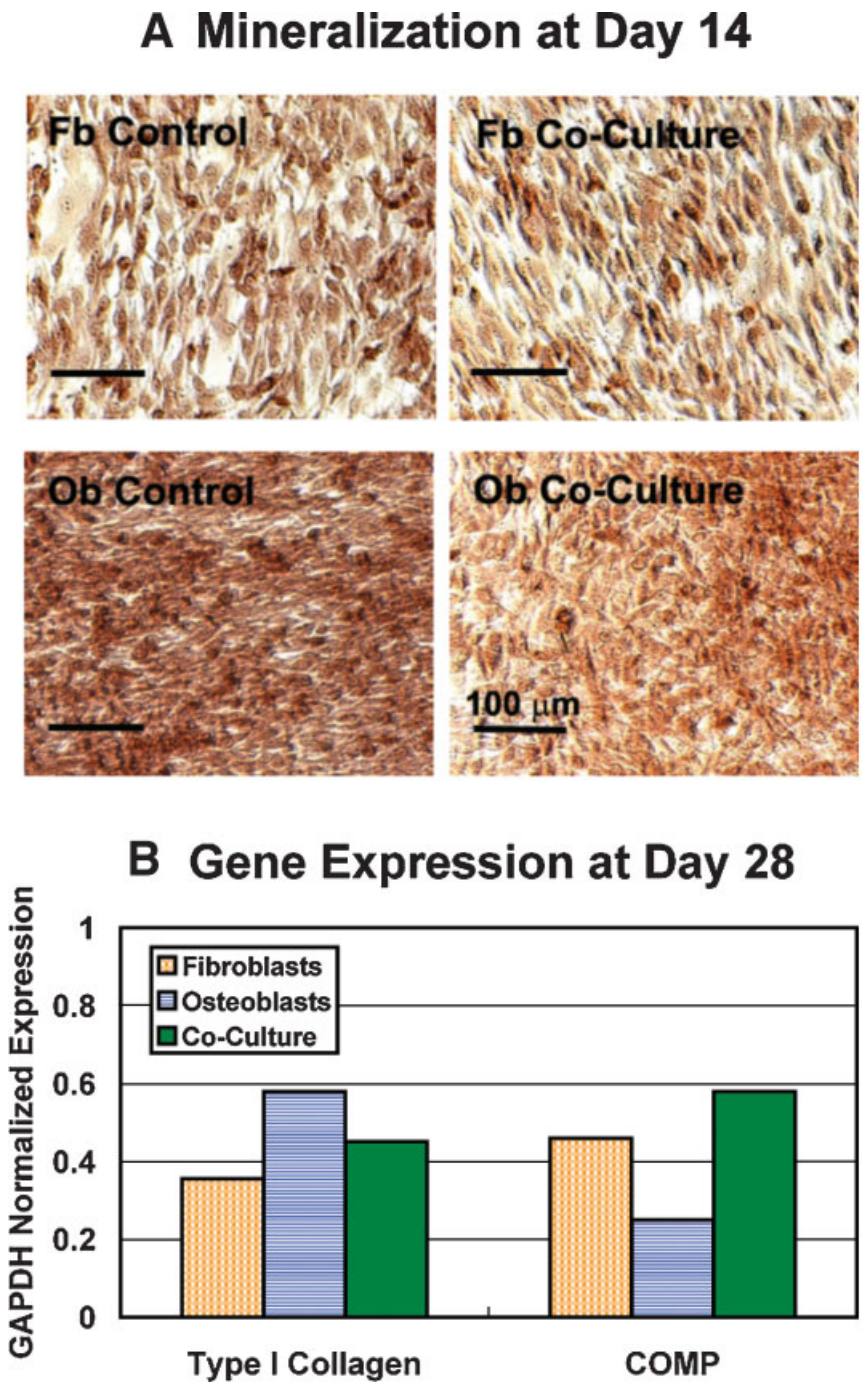

Figure 5. Effects of co-culture on mineralization and gene expression for interface-relevant markers. Osteoblasts (Ob) mineralization decreased in co-culture, while minimal mineralization was observed in the fibroblast (Fb) region of the co-cultured well. Co-culture resulted in the expression of several interface-relevant markers such as collagen types I as well as COMP. Gene expressions were normalized by GAPDH expression. (A) Alizarin Red S staining, day 14. (B) Gene expressions in all groups, day 28.

soluble factors. Cell migration following divider removal resulted in direct cell–cell physical contact, effectively establishing three distinct yet continuous cellular regions in co-culture: fibroblast-only, fibroblasts and osteoblasts, and osteoblast-only. This is reminiscent of the tendon-to-bone healing environment post ACL reconstruction, and is designed to investigate the collective effects of direct physical contact and paracrine signaling between fibroblasts and osteoblasts.

 DOI 10.1002/jor

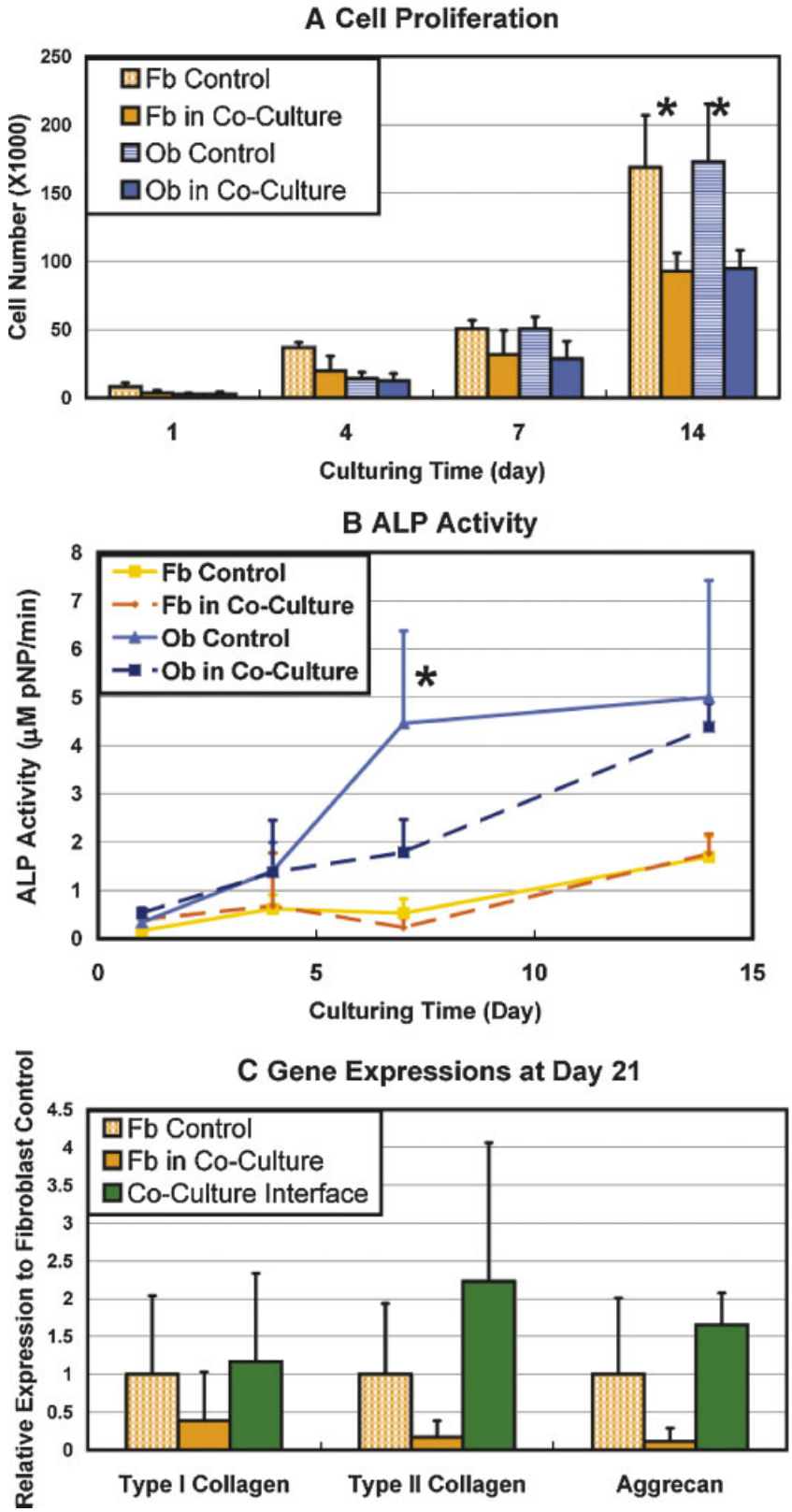

Figure 6. Response of cell subpopulations in co-culture. Co-culture significantly decreased fibroblast (Fb) as well as osteoblast (Ob) proliferations. Osteoblast alkaline phosphatase (ALP) activity was also delayed in co-culture. When compared to the fibroblasts-only control, cells (osteoblasts + fibroblasts) located at the interface region expressed relatively higher levels of collagen type II and aggrecan. (A) Fibroblast and osteoblast proliferation in co-culture. (B) Fibroblast and osteoblast ALP activity in co-culture. (C) Gene expression in co-culture relative to fibroblast-only control, day 21. (* denotes significance at $p < 0.05$).

After formulating the optimal media for co-culture, the model was used to evaluate the effects of osteoblast and fibroblast interactions. Our results suggest that co-culture induces significant changes in cell phenotypes, and leads to the expression of interface-relevant markers.

Both osteoblasts and fibroblasts proliferated in co-culture; however, their growth was delayed, suggesting mitogenic suppression due to heterotypic cellular interactions. As the fibroblast growth rate was higher than that of osteoblasts, to ensure that the observed response was not dominated by fibroblasts, an experiment was performed whereby the number of osteoblasts was doubled in co-culture. Increased osteoblast presence in co-culture significantly reduced cell proliferation (Fig. 3B), indicating that the observed growth suppression is likely mediated by osteoblasts. In addition, significant delays in both osteoblast ALP activity and mineralization were observed in co-culture. Ogiso et al. reported that conditioned media from periodontal ligament fibroblasts inhibited the ALP activity of bone marrow stromal cells, and this effect was mediated by paracrine factors such as prostaglandins.[29] A similar mechanism of interaction may exist here between the fibroblasts and osteoblasts and will be investigated in future studies. In this study, fibroblast ALP activity increased due to co-culture with osteoblasts, and this response was specific to fibroblasts based on the cell-tracking results. While only localized fibroblast mineralization was observed in co-culture, this may become significant over time. Taken collectively, these observations suggest that interactions between fibroblasts and osteoblasts suppress osteoblast ALP activity while enhancing fibroblast mineralization potential. These changes may represent initial indicators of fibroblast trans-differentiation due to co-culture.

Osteoblast–fibroblast interactions lead to the expression of interface-relevant markers. Interestingly, analysis of the interface region in the optimized model revealed that compared to the fibroblast control, collagen type II and aggrecan expressions were both up-regulated. A low level of collagen type II expression was also seen in the primary osteoblast control, which may reflect heterogeneity of the explant-derived osteoblast population (data not shown). The up-regulation of cartilage oligomeric matrix protein (COMP), a protein previously identified at the insertion[8] was also observed in co-culture. These results collectively provide evidence that osteoblast–fibroblast interactions may initiate fibrocartilage formation.

The current study focuses on osteoblast–fibroblast interactions, while the interface consists of chondrocytes embedded within a fibrocartilage matrix. Jiang et al. evaluated osteoblast and chondrocyte interactions using a monolayer-micromass model.[25] This co-culture model permits direct physical contact between these two cell types, while maintaining the required 3-D chondrocyte culture using the micromass. Similar to findings of the current study, osteoblast mineralization potential was significantly reduced due to heterotypic cellular interactions.[30] It is likely that osteoblast–fibroblast and osteoblast-chondrocyte interactions are key modulators of cell phenotypes at the graft-to-bone junction. This study used immature cells, as ACL injuries are reported to occur in the 15–35-years-old age group,[31] thus many of the patients are still skeletally immature. Future studies will focus on exploring the role of these heterotypic cellular interactions, as well as age-dependent effects on interface formation.

To our knowledge, this article is the first reported study to evaluate the role of cellular interactions in directing fibrocartilage formation using an in vitro co-culture model of the graft-to-bone interface. While it is promising that osteoblast–fibroblast interactions resulted in phenotypic changes and the expression of interface-relevant markers, a fibrocartilage-like interface was not formed in vitro during the culture period examined. It is likely that other cell types such as fibrochondrocyte precursors or mesenchymal stem cells are important for interface formation.[17,23,32] In vivo cell-tracking studies have reported that post ACL reconstruction, the tendon graft is populated by host cells within 1 week.[17,33] When Lim et al.[34] coated tendon grafts with mesenchymal stem cells embedded in a fibrin gel, the formation of a zone of cartilaginous tissue between graft and bone was observed, suggesting a potential role for these stem cells in interface formation. It is likely that osteoblast–fibroblast interactions may also direct the fibrochondrogenic differentiation of the progenitor cells or mesenchymal stem cells. Future work will focus on applying this novel co-culture model to test this working hypothesis and further elucidate the role of osteoblast–fibroblast interactions in fibrocartilage formation and interface formation.

CONCLUSIONS

We have designed and optimized a biomimetic co-culture model and have subsequently utilized this model to evaluate the role of osteoblast–fibroblast

interactions in initiating fibrocartilage formation. Co-culture of fibroblasts and osteoblasts leads to changes in their respective phenotypes as well as the expression of interface-relevant markers. The findings of this study provide initial confirmation of the role of osteoblast–fibroblast interactions in fibrocartilage formation, and demonstrate the utility of in vitro co-culture models for investigating the mechanism governing the formation of the soft tissue-to-bone interface.

ACKNOWLEDGMENTS

The authors thank Ashby O. Thomas of Columbia University for assistance with RT-PCR (COMP), and Jones Tsai of Columbia University for assistance with cell labeling. This study was funded by NIH-NIAMS (AR052402-01A1; H. H. L.) and the Wallace H. Coulter Foundation (H. H. L.).

REFERENCES

1. Cooper RR, Misol S. 1970. Tendon and ligament insertion. A light and electron microscopic study. J Bone Joint Surg [Am] 52:1–20.
2. Benjamin M, Evans EJ, Copp L. 1986. The histology of tendon attachments to bone in man. J Anat 149:89–100.
3. Niyibizi C, Visconti CS, Kavalkovich K, et al. 1995. Collagens in an adult bovine medial collateral ligament: immunofluorescence localization by confocal microscopy reveals that type XIV collagen predominates at the ligament-bone junction. Matrix Biol 14:743–751.
4. Wei X, Messner K. 1996. The postnatal development of the insertions of the medial collateral ligament in the rat knee. Anat Embryol (Berl) 193:53–59.
5. Messner K. 1997. Postnatal development of the cruciate ligament insertions in the rat knee. Morphological evaluation and immunohistochemical study of collagens types I and II. Acta Anat (Basel) 160:261–268.
6. Petersen W, Tillmann B. 1999. Structure and vascularization of the cruciate ligaments of the human knee joint. Anat Embryol (Berl) 200:325–334.
7. Thomopoulos S, Williams GR, Gimbel JA, et al. 2003. Variations of biomechanical, structural, and compositional properties along the tendon to bone insertion site. J Orthop Res 21:413–419.
8. Wang IE, Mitroo S, Chen FH, et al. 2006. Age-dependent changes in matrix composition and organization at the ligament-to-bone insertion. J Orthop Res 24:1745–1755.
9. Kurosaka M, Yoshiya S, Andrish JT. 1987. A biomechanical comparison of different surgical techniques of graft fixation in anterior cruciate ligament reconstruction. Am J Sports Med 15:225–229.
10. Rodeo SA, Arnoczky SP, Torzilli PA, et al. 1993. Tendon-healing in a bone tunnel. A biomechanical and histological study in the dog. J Bone Joint Surg [Am] 75:1795–1803.
11. Rodeo SA, Suzuki K, Deng XH, et al. 1999. Use of recombinant human bone morphogenetic protein-2 to enhance tendon healing in a bone tunnel. Am J Sports Med 27:476–488.
12. Friedman MJ, Sherman OH, Fox JM, et al. 1985. Autogeneic anterior cruciate ligament (ACL) anterior reconstruction of the knee. A review. Clin Ortho Relat Res 196:9–14.
13. Robertson DB, Daniel DM, Biden E. 1986. Soft tissue fixation to bone. Am J Sports Med 14:398–403.
14. Yahia L. 1997. Ligaments and ligamentoplasties Berlin/Heidelberg: Springer-Verlag.
15. Niyibizi C, Sagarrigo VC, Gibson G, et al. 1996. Identification and immunolocalization of type X collagen at the ligament-bone interface. Biochem Biophys Res Commun 222:584–589.
16. Woo SL, Buckwalter JA. 1988. AAOS/NIH/ORS workshop. Injury and repair of the musculoskeletal soft tissues. Savannah, Georgia, June 18-20, 1987. J Orthop Res 6:907–931.
17. Lu HH, Jiang J. 2006. Interface tissue engineering and the formulation of multiple-tissue systems. Adv Biochem Eng Biotechnol 102:91–111.
18. Fujioka H, Thakur R, Wang GJ, et al. 1998. Comparison of surgically attached and non-attached repair of the rat Achilles tendon-bone interface. Cellular organization and type X collagen expression. Connect Tissue Res 37:205–218.
19. Blickenstaff KR, Grana WA, Egle D. 1997. Analysis of a semitendinosus autograft in a rabbit model. Am J Sports Med 25:554–559.
20. Yoshiya S, Nagano M, Kurosaka M, et al. 2000. Graft healing in the bone tunnel in anterior cruciate ligament reconstruction. Clin Ortho Relat Res 376:278–286.
21. Eriksson K, Kindblom LG, Wredmark T. 2000. Semitendinosus tendon graft ingrowth in tibial tunnel following ACL reconstruction: a histological study of 2 patients with different types of early graft failure. Acta Orthop Scand 71:275–279.
22. Lu HH, Cooper JA Jr, Manuel S, et al. Anterior cruciate ligament regeneration using braided biodegradable scaffolds: in vitro optimization studies. Biomaterials 26:4805–4816.
23. Spalazzi JP, Doty SB, Moffat KL, et al. 2006. Development of controlled matrix heterogeneity on a triphasic scaffold orthopedic interface tissue engineering. Tissue Eng 12:3497–3508.
24. Spalazzi JP, Dionisio KL, Jiang J, et al. 2003. Osteoblast and chondrocyte interactions during coculture on scaffolds. IEEE Eng Med Biol Mag 22:27–34.
25. Jiang J, Nicoll SB, Lu HH. 2005. Co-culture of osteoblasts and chondrocytes modulates cellular differentiation in vitro. Biochem Biophys Res Commun 338:762–770.
26. Lu HH, Tang A, Oh SC, et al. 2005. Compositional effects on the formation of a calcium phosphate layer and the response of osteoblast-like cells on polymer-bioactive glass composites. Biomaterials 26:6323–6334.
27. Sun Y, Kandel R. 1999. Deep zone articular chondrocytes in vitro express genes that show specific changes with mineralization. J Bone Miner Res 14:1916–1925.
28. Bosnakovski D, Mizuno M, Kim G, et al. 2004. Chondrogenic differentiation of bovine bone marrow mesenchymal stem cells in pellet cultural system. Exp Hematol 32:502–509.
29. Ogiso B, Hughes FJ, Melcher AH, et al. 1991. Fibroblasts inhibit mineralised bone nodule formation by rat bone

marrow stromal cells in vitro. J Cell Physiol 146:442–450.
30. Jiang J, Leong NL, Mung JC, et al. 2007. Interaction between zonal populations of articular chondrocytes suppresses chondrocyte mineralization and this process is mediated by PTHrP. Osteoarthritis Cartilage (in press).
31. Seil R, Kohn D. 2000. Ruptures of the anterior cruciate ligament (ACL) during growth. Bull Soc Sci Med Grand Duche Luxemb 1:39–53.
32. Mikos AG, Herring SW, Ochareon P, et al. 2006. Engineering complex tissues. Tissue Eng 12:3307–3339.
33. Kobayashi M, Watanabe N, Oshima Y, et al. 2005. The fate of host and graft cells in early healing of bone tunnel after tendon graft. Am J Sports Med 33:1892– 1897.
34. Lim JK, Hui J, Li L, et al. 2004. Enhancement of tendon graft osteointegration using mesenchymal stem cells in a rabbit model of anterior cruciate ligament reconstruction. Arthroscopy 20:899–910.

 DOI 10.1002/jor